Theory of effective g factors and effective masses in diluted magnetic semiconductors

R. L. Hota and G. S. Tripathi
Department of Physics, Berhampur University, Berhampur-760007, Orissa, India

J. N. Mohanty
Department of Physics, Ravenshaw College, Cuttack-753003, Orissa, India
(Received 4 August 1992; revised manuscript received 13 November 1992)

We derive an expression for the effective g factor in the presence of magnetic impurities. The expression is suitably modified as to make it applicable to diluted magnetic semiconductors. We calculate the effective g factors and effective masses in $Pb_{1-x}Mn_xTe$ and $Pb_{1-x}Mn_xSe$ using a $\mathbf{k}\cdot\boldsymbol{\pi}$ band model developed and used previously for nonmagnetic ternary semiconductors by us. It is found that, while the exchange interaction between the conduction electrons and the magnetic impurities contributes significantly to the effective g factor, the exchange effects are marginal in the case of effective masses. Both quantities are calculated for the band edges, as well as for different carrier concentrations, as functions of magnetic-impurity concentration. The calculated results and trends obtained are in overall agreement with experimental results where available. The expression for the effective g factor derived is general in the sense that it can be applied to other diluted magnetic semiconductors with suitable modifications.

I. INTRODUCTION

Diluted magnetic semiconductors (DMS) form an important class of magnetic materials. These are semiconducting alloys whose lattice is made up in part of substitutional magnetic atoms. A typical DMS is represented by the chemical formula $A_{1-x}M_xB$, where AB represents a binary nonmagnetic semiconductor and M is a magnetic-impurity atom that enters the lattice substitutionally replacing the A atom of the AB semiconductor. Although the effect of magnetic impurities on semiconductors was studied as early as the early 70s,[1] only recently the study of these semiconductors is intensified, as evidenced by the large number of articles published in recent years.[2–5] Among these semiconductors, the systems of type $A^{II}_{1-x}Mn_xB^{VI}$ are the most extensively studied and most thoroughly understood ones. However, the physics of the semimagnetic semiconductors involving IV–VI compounds has recently attracted considerable attention. A lot of experimental work is now available[6–17] on these systems which include $Pb_{1-x}Mn_xTe$, $Pb_{1-x}Mn_xSe$, $Pb_{1-x}Gd_xTe$, $Pb_{1-x}Eu_xTe$, $Pb_{1-x}Mn_xS$, etc. On the other hand, very little theoretical work has been done on these systems.[18,19]

It is well known that the subject of magnetic impurities in metals is rich, fascinating, and well investigated. In contrast, the magnetic-impurity problem in semiconductors is of recent origin. But the experimental data on these materials indicate that the physics of semimagnetic semiconductors would be equally interesting and intellectually satisfying. It has been found that, with the change of magnetic content x over a wide range, some of these systems exhibit different magnetic states like diamagnetic, paramagnetic, spin glass, and anti-ferromagnetic states, in succession.[2,3]

In order to understand the physics of these interesting magnetic materials, we have undertaken an investigation in this work of the effective g factors and effective masses in $Pb_{1-x}Mn_xTe$ and $Pb_{1-x}Mn_xSe$. The lead salts are narrow-gap multiband systems with a large spin-orbit interaction. These semiconductors are highly diamagnetic and have large g factors compared to the free-electron g values. It has also been seen that g values are enhanced when these semiconductors are alloyed with tin telluride.[20] We are interested in seeing how these g factors are modified with an increase in magnetic impurities in these semiconductors.

While expressions for the effective g factor exist for nonmagnetic semiconductors,[21,22] the g factors in the diluted magnetic semiconductors are calculated using simplified and intuitive formulas.[23–25] Since the mean magnetic moments of the impurities are functions of temperature and change with magnetic field, in a diluted magnetic semiconductor the effective g factor is an essentially temperature-, magnetic-field-, and magnetic-component-concentration-dependent quantity. Furthermore, the strong temperature and the magnetic-field dependence of the g factor is believed to be responsible for the exotic temperature dependence of the quantum oscillation amplitude in the DMS's.[26–28] In view of the importance of the effective g factor in the understanding of different phenomena in the DMS's, we present in this work a careful analysis of the effective g factors by first deriving an expression for the effective g factors in the presence of magnetic impurities and then applying it to $Pb_{1-x}Mn_x$(Te,Se). We also derive expressions for the effective masses and cyclotron mass anisotropies for these semiconductors.

This work is organized in the following way. In Sec. II, we derive an expression for the effective g factor in the presence of magnetic impurities. In Sec. III, we present our calculations of the effective g factors in $Pb_{1-x}Mn_x$(Te,Se) and study the effects of the exchange interaction between the carriers and magnetic impurities on the effective g factor. The g-factor variation with carrier densities is also analyzed in the same section. The

aforesaid calculations and analysis were done using a $\mathbf{k}\cdot\boldsymbol{\pi}$ band model previously developed and used by us. In Sec. IV, we derive expressions for the effective masses and cyclotron mass anisotropies and calculate these quantities for the above-mentioned systems. A summary of the results followed by an appropriate conclusion is presented in Sec. V. In the Appendix, we present an alternative derivation of the effective g factor from the expression for the Knight shift in the presence of magnetic impurities.

II. THEORY OF EFFECTIVE g FACTOR

The one-electron Hamiltonian in a periodic potential $V(\mathbf{r})$, spin-orbit interaction, uniform magnetic field $\mathbf{B}$, and exchange interaction $\mathcal{H}_{ex}$ is

$$\mathcal{H}=\frac{1}{2m}\left[\mathbf{p}+\frac{e}{c}\mathbf{A}\right]^2+V(\mathbf{r}) +\frac{\hbar}{4m^2c^2}\boldsymbol{\sigma}\cdot\left[\nabla V\times\left[\mathbf{p}+\frac{e}{c}\mathbf{A}\right]\right] +\tfrac{1}{2}g_0\mu_0\mathbf{B}\cdot\boldsymbol{\sigma}+\mathcal{H}_{\rm ex}\ , \tag{2.1}$$

where

$$\mathcal{H}_{\rm ex}=\tfrac{1}{2}\sum_{\mathbf{R}_i}\mathcal{J}(\mathbf{r}-\mathbf{R}_i)\mathbf{J}_i\cdot\boldsymbol{\sigma}\ . \tag{2.2}$$

In Eqs. (2.1) and (2.2), $A(\mathbf{r})$ is the vector potential, g_0 is the free-electron g factor, μ_0 is the Bohr magneton, $\boldsymbol{\sigma}$ is the Pauli spin operator, $\mathcal{J}$ is the exchange interaction function, $\mathbf{J}_i$ is the total angular momentum operator of the ith magnetic ion, and $\mathbf{r}$ and $\mathbf{R}_i$ define the coordinates of the band electron and the ith ion, respectively. The other symbols have their usual meanings. The eigenfunctions of the unperturbed Hamiltonian ($\mathbf{B}=0$, $\mathcal{H}_{\rm ex}=0$) are the Bloch functions

$$\psi_{n\mathbf{k}\rho}(\mathbf{r})=e^{i\mathbf{k}\cdot\mathbf{r}}U_{n\mathbf{k}\rho}(\mathbf{r})\ , \tag{2.3}$$

where $U_{n\mathbf{k}\rho}$ is a periodic two-component function, n is the band index, $\mathbf{k}$ is the reduced wave vector, and the index $\rho,\rho=1,2$, distinguishes the two independent eigenfunctions $\psi_{n,\mathbf{k},1}$ and $\psi_{n,\mathbf{k},2}$ which belong to a general wave vector $\mathbf{k}$ and energy $E_n(\mathbf{k})$ if the crystal has inversion symmetry.

Since the Bloch functions form an orthonormal complete set, the wave function for an eigenstate of our problem, $\psi(\mathbf{r})$, can be expanded as

$$\psi(\mathbf{r})=\sum_{n\mathbf{k}\rho}\psi_{n\mathbf{k}\rho}(\mathbf{r})\phi_{n,\rho}(\mathbf{k})\ , \tag{2.4}$$

where $\phi_{n,\rho}(\mathbf{k})$ are the expansion coefficients and are periodic in $\mathbf{k}$. $\psi(\mathbf{r})$ satisfies the equation

$$\mathcal{H}\psi(\mathbf{r})=E\psi(\mathbf{r})\ . \tag{2.5}$$

Since band electrons interact simultaneously with a large number of magnetic ions, the operator $\mathbf{J}_i$ can be replaced by its thermal average $\langle\mathbf{J}_i\rangle$ in the molecular field approximation. Moreover, the large extension of the Bloch function makes it possible to write Eq. (2.2) in the virtual crystal approximation as

$$\mathcal{H}_{\rm ex}=\tfrac{1}{2}xN_s\langle J^\mu\rangle\sigma^\mu\mathcal{J}(\mathbf{r})\ , \tag{2.6}$$

where x is the fraction of magnetic ions in the DMS lattice and N_s is the number of unit cells in the unit volume. μ represents Cartesian components and repeated indices here and elsewhere in the paper μ implies summation.

Following the standard procedure in the crystal momentum representation,[29] we obtain the effective equation of motion in $\mathbf{k}$ space:

$$\mathcal{H}(\boldsymbol{\kappa})\phi(\mathbf{k})=E\phi(\mathbf{k})\ , \tag{2.7}$$

where $\mathcal{H}(\boldsymbol{\kappa})$ is the effective Hamiltonian,

$$\mathcal{H}(\boldsymbol{\kappa})=\frac{1}{2m}(\mathbf{p}+\hbar\boldsymbol{\kappa})^2+V+\frac{\hbar}{4m^2c^2}\boldsymbol{\sigma}\cdot\nabla V\times(\mathbf{p}+\hbar\boldsymbol{\kappa}) +\tfrac{1}{2}g_0\mu_0B^\mu\sigma^\mu+\tfrac{1}{2}xN_s\langle J^\mu\rangle\sigma^\mu\mathcal{J}\ , \tag{2.8}$$

where

$$\boldsymbol{\kappa}=\mathbf{k}+i\mathbf{h}\times\nabla_{\mathbf{k}},\quad \mathbf{h}=e\mathbf{B}/2\hbar c\ . \tag{2.9}$$

Using Eq. (2.9) in Eq. (2.8) and retaining terms first order in the magnetic field, we obtain the effective Zeeman Hamiltonian $\mathcal{H}_z^{\rm eff}(\mathbf{k})$:

$$\mathcal{H}(\boldsymbol{\kappa})=\mathcal{H}_0(\mathbf{k})+\mathcal{H}_z^{\rm eff}(\mathbf{k})\ , \tag{2.10}$$

where $\mathcal{H}_0(\mathbf{k})$ is the unperturbed Hamiltonian:

$$\mathcal{H}_0(\mathbf{k})=\frac{1}{2m}(\mathbf{p}+\hbar\mathbf{k})^2+V+\frac{\hbar}{4m^2c^2}\boldsymbol{\sigma}\cdot\nabla V\times(\mathbf{p}+\hbar\mathbf{k}) \tag{2.11}$$

and

$$\mathcal{H}_z^{\rm eff}(\mathbf{k})=\tfrac{1}{2}g_0\mu_0B^\mu\sigma^\mu-i\frac{\hbar}{m}h_{\alpha\beta}\pi^\alpha\nabla_k^\beta+\tfrac{1}{2}xN_s\langle J^\mu\rangle\sigma^\mu\mathcal{J}\ . \tag{2.12}$$

In Eq. (2.12),

$$h_{\alpha\beta}=\epsilon_{\alpha\beta\mu}h^\mu\ , \tag{2.13}$$

where $\epsilon_{\alpha\beta\mu}$ is an antisymmetric tensor of third rank and we follow the Einstein summation convention.

The effective Zeeman Hamiltonian for the nth band is

$$\mathcal{H}_{zn\rho,n\rho}^{\rm eff}=\tfrac{1}{2}\mu_0g_{nn}^{{\rm eff},\mu}B^\mu\ , \tag{2.14}$$

where $g_{nn}^{{\rm eff},\mu}$ is the μth component of effective g factor for the nth band. Also, from Eq. (2.12), we obtain

$$\mathcal{H}_{zn\rho,n\rho}^{\rm eff}(\mathbf{k})=\tfrac{1}{2}g_0\mu_0B^\mu\sigma_{n\rho,n\rho}^\mu(\mathbf{k})-i\frac{\hbar}{m}h_{\alpha\beta}(\pi^\alpha\nabla_{\mathbf{k}}^\beta)_{\eta\rho,\eta\rho} +\tfrac{1}{2}xN_s\langle J^\mu\rangle(\sigma^\mu\mathcal{J})_{n\rho,n\rho}\ . \tag{2.15}$$

Using the completeness property of the $U_{n\mathbf{k}\rho}$'s and Eqs. (2.9) and (2.13), the second term of Eq. (2.15) can be written as

$$-i\frac{\hbar}{m}h_{\alpha\beta}(\pi^\alpha\nabla_{\mathbf{k}}^\beta)_{n\rho,n\rho}=-i\frac{\hbar}{m}\frac{eB^\mu}{2\hbar c}\sum_{\substack{m\rho'\\ m\neq n}}\langle n\rho|\pi^\alpha|m\rho'\rangle \times\langle m\rho'|\nabla_{\mathbf{k}}^\beta|n\rho\rangle\ , \tag{2.16}$$

which, using the identity[30]

$$\langle m\rho'|\nabla_{\mathbf{k}}^{\beta}|n\rho\rangle=\frac{\hbar}{m}\frac{\pi^{\beta}_{m\rho',n\rho}}{E_{nm}} ,$$

can be written as

$$-i\frac{\hbar}{m}h_{\alpha\beta}(\pi^{\alpha}\nabla_{\mathbf{k}}^{\beta})_{n\rho,n\rho}$$
$$=i\frac{\mu_0 B^{\mu}}{m}\epsilon_{\alpha\beta\mu}\sum_{m\rho'}\frac{\pi^{\alpha}_{n\rho,m\rho'}\pi^{\beta}_{m\rho',n\rho}}{E_{mn}} . \quad (2.17)$$

Using Eq. (2.17) in Eq. (2.15), we obtain

$$\mathcal{H}^{\text{eff}}_{zn\rho,n\rho}(\mathbf{k})=\tfrac{1}{2}\mu_0\left[g_0\sigma^{\mu}_{n\rho,n\rho}(\mathbf{k})+\frac{2i}{m}\epsilon_{\alpha\beta\mu}\sum_{\substack{m\rho'\\ m\neq n}}\frac{\pi^{\alpha}_{n\rho,m\rho'}\pi^{\beta}_{m\rho',n\rho}}{E_{mn}}+xN_s\frac{\langle J^{\mu}\rangle}{\mu_0 B^{\mu}}(\sigma^{\mu}\mathcal{J})_{n\rho,n\rho}\right]B^{\mu} . \quad (2.18)$$

Comparing Eqs. (2.14) and (2.18), we obtain

$$g^{\text{eff},\mu}_{nn}(\mathbf{k})=g_0\sigma^{\mu}_{n\rho,n\rho}+\frac{2i}{m}\epsilon_{\alpha\beta\mu}\sum_{\substack{m\rho'\\ m\neq n}}\frac{\pi^{\alpha}_{n\rho,m\rho'}\pi^{\beta}_{m\rho',n\rho}}{E_{mn}}+xN_s\frac{\langle J^{\mu}\rangle}{\mu_0 B^{\mu}}(\sigma^{\mu}\mathcal{J})_{n\rho,n\rho} . \quad (2.19)$$

This is an expression for the effective g factor in the presence of magnetic impurities. In the absence of magnetic impurities, it reduces to the familiar expression for the effective g factor, $g^{\text{eff},\mu}_{nn,0}(\mathbf{k})$, derived earlier by one of the authors.[30] Thus, Eq. (2.19) can be written as

$$g^{\text{eff},\mu}_{nn}(\mathbf{k})=g^{\text{eff},\mu}_{nn,0}(\mathbf{k})+g^{\text{eff},\mu}_{nn,i}(\mathbf{k}) , \quad (2.20)$$

where

$$g^{\text{eff},\mu}_{nn,i}(\mathbf{k})=xN_s\frac{\langle J^{\mu}\rangle}{\mu_0 B^{\mu}}(\sigma^{\mu}\mathcal{J})_{n\rho,n\rho} . \quad (2.21)$$

Thus is the effective g factor due to the interaction of the conduction electrons with the magnetic impurities. Equation (2.20) is same as the formulas used previously[2,23,24] but derived in a more systematic way. In the Appendix, we give an alternative derivation of Eq. (2.19) from the expression for the Knight shift,[31,32] thus showing the dependence of this quantity on the effective g factor.

III. EFFECTIVE g FACTORS IN PbMnTe AND PbMnSe

Lead salt semiconductors (PbTe, PbSe, and PbS) crystallize in rock-salt crystal structure and the minimum energy gap in these semiconductors is direct and occurs at the L point of the Brillouin zone. The energy level diagrams at the L point for PbTe and PbSe are shown in Fig. 1. These levels are described by the Mitchell-Wallis (MW) basis wave functions[30] and we list below one of Kramer's conjugate pairs for each level:

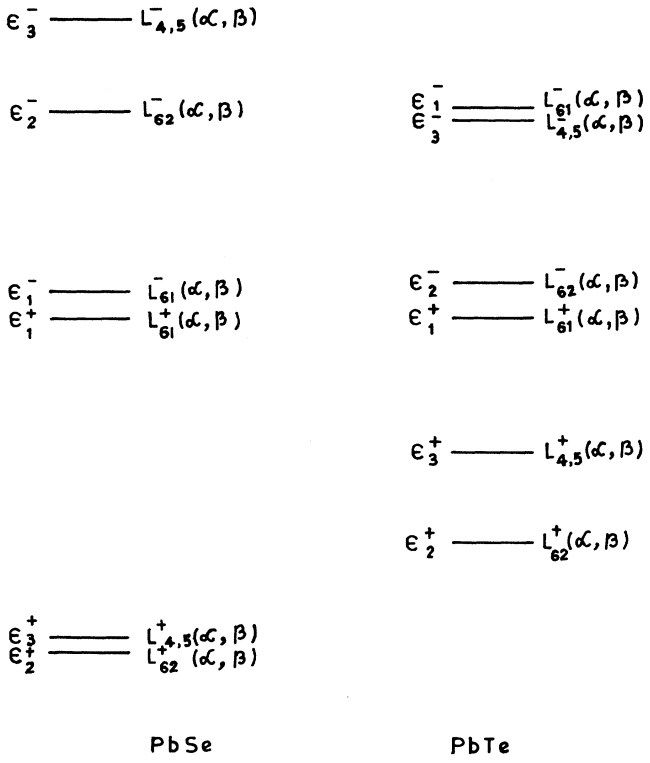

FIG. 1. Energy level diagrams at the L point for PbTe and PbSe. $-$ and $+$ signs represent conduction and valence bands, respectively.

$$\begin{aligned}
L^-_{61}\alpha&=\cos\theta^- Z\uparrow-\sin\theta^- X_+\downarrow ,\\
L^-_{5}\alpha&=\frac{1}{\sqrt{2}}(-X_-\downarrow+iX_+\uparrow) ,\\
L^-_{62}\alpha&=\sin\theta^- Z\uparrow+\cos\theta^- X_+\downarrow ,\\
L^+_{61}\alpha&=-i\cos\theta^+ R\uparrow-\sin\theta^+ S_+\downarrow ,\\
L^+_{5}\alpha&=\frac{1}{\sqrt{2}}(S_-\downarrow+iS_+\uparrow) ,
\end{aligned} \quad (3.1)$$

and

$$L^+_{62}\alpha=i\sin\theta^+ R\uparrow+\cos\theta^+ S_+\downarrow ,$$

where $\cos\theta^{\pm}$ and $\sin\theta^{\pm}$ are the amplitudes of single group wave functions in the double group wave functions. The spatial parts of these basis functions have the following transformation properties about Pb: R transforms like an atomic s state, $X_{\pm}$ and Z transform like atomic p functions with $m_z=\pm1$ and 0, and $S_{\pm}$ transform like atomic d functions with $m_z=\pm1$. The ordering of the levels is followed from Bernick and Kleinman.[34]

We follow a $\mathbf{k}\cdot\boldsymbol{\pi}$ band model to evaluate the g factors. In this approach the band edge states are treated exactly and the far band effects are considered using perturbation theory. The details of these methods are discussed in our earlier works.[30,35–37] The dispersion relations for the conduction and valence bands are[20]

$$E_{c,v}(\mathbf{k})=\epsilon_{c,v}+\frac{\hbar^2k^2}{2m}\pm\tfrac{1}{2}E_G(W-1)+M_{1c,v}k_\rho^2+M_{2c,v}k_z^2+\left[\frac{M_{3c,v}}{W(1+W)}+\frac{M_{4c,v}}{W}\right]k_\rho^4+\left[\frac{M_{5c,v}}{W(1+W)}+\frac{M_{6c,v}}{W}\right]k_z^4+\left[\frac{M_{7c,v}}{W(1+W)}+\frac{M_{8c,v}}{W}\right]k_\rho^2k_z^2\ , \tag{3.2}$$

where

$$W=\sqrt{1+\alpha k_\rho^2+\beta k_z^2}\ , \tag{3.3}$$

$$\alpha=2\frac{\hbar^2s^2}{m^2E_G^2}\ , \tag{3.4}$$

$$\beta=4\frac{\hbar^2t^2}{m^2E_G^2}\ , \tag{3.5}$$

$$k_\rho^2=k_x^2+k_y^2\ , \tag{3.6}$$

$$s=\langle L_{61}^{+}\alpha|\pi^{+}|L_{62}^{-}\beta\rangle=\langle L_{61}^{+}\beta|\pi^{-}|L_{62}^{-}\alpha\rangle\ , \tag{3.7}$$

and

$$t=-\langle L_{61}^{+}\alpha|\pi^{z}|L_{62}^{-}\alpha\rangle=\langle L_{61}^{+}\beta|\pi^{z}|L_{62}^{-}\beta\rangle\ . \tag{3.8}$$

$L_{c,v}^{\pm}\beta$ are the Kramers conjugates of $L_{c,v}^{\pm}\alpha$. E_G is the band gap at the L point; c and v in Eq. (3.2) denote the conduction and valence bands except in the third term in which case these are denoted by $+$ and $-$ signs. M_1 to M_8 are complicated functions of momentum matrix elements and energy gaps at the L point.[35]

The variation of the energy gap with Mn concentrations in $Pb_{1-x}Mn_xTe$ is considered using the formula[6]

$$\frac{dE_G}{dx}=0.048\ \text{eV}/\%\text{Mn},\quad 0<x<0.04 \tag{3.9}$$

and in $Pb_{1-x}Mn_xSe$ from a graphical analysis in Ref. 17. In both cases, at a given temperature, the energy gap increases with Mn concentration. While in the PbMnTe case, the variation is monotonic as seen in Eq. (3.9), in the PbMnSe case, it is almost monotonic up to $x=0.02$, then it slows down.[17]

In order to calculate the effective g factors, the single group momentum matrix elements are used from Ref. 37, which were calculated[38] within the framework of a psuedopotential band calculation.[34] The energy levels and $\sin\theta^{\pm}$ and $\cos\theta^{\pm}$ are taken from Bernick and Kleinman.[34] The exchange interaction matrix elements occurring in Eq. (2.21) are given below for the band edge states in PbMnSe:

$$A'=\langle L_{61}^{+}\alpha|\sigma^z\mathcal{A}(\mathbf{r})|L_{61}^{+}\alpha\rangle=\eta\cos^2\theta^{+}-\delta\sin^2\theta^{+} \tag{3.10}$$

and

$$B'=\langle L_{61}^{-}\alpha|\sigma^z\mathcal{A}(\mathbf{r})|L_{61}^{-}\alpha\rangle=\beta_{\parallel}\cos^2\theta^{-}-\beta_{\perp}\sin^2\theta^{-}\ , \tag{3.11}$$

where

$$\eta=\langle R|\mathcal{A}|R\rangle/\Omega_0\ , \tag{3.12a}$$

$$\delta=\langle S_+|\mathcal{A}|S_+\rangle/\Omega_0\ , \tag{3.12b}$$

$$\beta_{\parallel}=\langle Z|\mathcal{A}|Z\rangle/\Omega_0\ , \tag{3.12c}$$

and

$$\beta_{\perp}=\langle X_+|\mathcal{A}|X_+\rangle/\Omega_0\ . \tag{3.12d}$$

Ω_0 is the unit-cell volume. In the PbMnTe case, $L_{61}^{-}\alpha$ is replaced by $L_{62}^{-}\alpha$ in B'. The values of A' and B' for PbMnSe are taken from Ref. 17 and the same parameters for PbMnTe are used from Ref. 39. The exchange parameters are

$$\text{for PbMnSe:}\quad A'=(-0.08\pm0.01)\ \text{eV}\ ,\quad B'=(0.02\pm0.01)\ \text{eV}\ , \tag{3.13}$$

$$\text{for PbMnTe:}\quad A'=-0.45\ \text{eV}\ ,\quad B'=0.29\ \text{eV}\ . \tag{3.14}$$

The chemical potential is calculated, using a self-consistent method from the expression[35]

$$\mu=\mu'+\left[\mu-\frac{\hbar^2}{2m}(3\pi^2F)^{2/3}\right]\ , \tag{3.15}$$

where

$$F=\frac{8}{(2\pi)^3}\int f[E_{c,v}(\mathbf{k})-\mu]d^3k \tag{3.16}$$

and

$$\mu'=\frac{\hbar^2}{2m}(3\pi^2n)^{2/3}\ . \tag{3.17}$$

The factor 8 in Eq. (3.16) accounts for the spin degeneracies of the energy levels and the four L valleys of the Brillouin zone; μ' is the free-electron chemical potential and n is the concentration of carriers. Cylindrical coordinates are used for the evaluation of the integral in Eq. (3.16) and the integration is done numerically.

The details of the calculation of $g_{nn,0}^{\text{eff},\mu}(\mathbf{k})$ in Eq. (2.20) is discussed in Ref. 20. In order to evaluate $g_{nn,i}^{\text{eff},\mu}(\mathbf{k})$ we use the wave functions [Eqs. (3.7a)–(3.7d)] of Ref. 20 to evaluate $(\sigma^\mu\mathcal{A})_{n\rho,n\rho}$. When the field is along the Z direction, we have for Mn^{2+}

$$\langle J^z\rangle=\langle S^z\rangle=-S_0B_s(y) \tag{3.18}$$

and

$$\langle S^x\rangle=\langle S^y\rangle=0\ , \tag{3.19}$$

where S_0 is the maximum value of the spin, and

$$B_s(y)=\frac{2S+1}{2S}\coth\left[\frac{2S+1}{2S}y\right]-\frac{1}{2S}\coth\left[\frac{1}{2S}y\right] \tag{3.20}$$

with

$$y=\frac{g_i\mu_0SB}{K_BT}\ , \tag{3.21}$$

g_i and S being the Lande g factor and the spin of the im-

purity ion, respectively. The effective g factors are calculated for band edge states and for different carrier densities as a function of manganese concentrations using the formula

$$g_{nn}^{\text{eff}}=\tfrac{1}{3}g_{nn,0}^{\text{eff},l}+\tfrac{2}{3}g_{nn,0}^{\text{eff},t}+g_{nn,i}^{\text{eff},z}\ , \tag{3.22}$$

where l and t represent the components of the effective g factor along crystallographic [111] and $[\bar{1}\,\bar{1}2]$ or $[1\bar{1}0]$ directions, Z represents [001]. The conduction-band and valence-band effective g factors are given, respectively, by

$$g_c^{\text{eff}}=g_{c,0}+g_{c,i} \tag{3.23}$$

and

$$g_v^{\text{eff}}=g_{v,0}+g_{v,i}\ , \tag{3.24}$$

where $g_{c,0}$ and $g_{v,0}$ are the g factors in the absence of exchange interactions and are given in Ref. 20. The band edge values are calculated for $k_\rho^2=0$ and $k_z^2=0$. For arbitrary carrier densities the g values are calculated by substituting k_z by its Fermi surface value k_l, which is obtained by solving the equation

$$E_{c,v}(k_\rho^2,k_l)-\mu=0 \tag{3.25}$$

for $k_\rho^2=0$.

In Table I, we have listed the band edge g values for different values of x. In both n- and p-type $Pb_{1-x}Mn_xSe$, the g values without exchange decrease with an increase in x. However, while the exchange contribution to the g factor for the p-type system is $+ve$ and increases with x, thus causing an overall increase of g values with x, the same contribution for the n-type system is $-ve$ and increases with x, thus, reducing the overall g values with increase in x. A comparison of calculated values and experimental results,[17] where available, shows fairly good agreement. In Fig. 2, we have plotted the g values, for different Mn concentrations, as functions of the carrier density. For fixed values of x the g values decrease with an increase in carrier density. However, unfortunately, we are not aware of any experimental values for comparison. All these calculations are done at 4.2 K since the variation of the energy gap with x is available only at this temperature.[17]

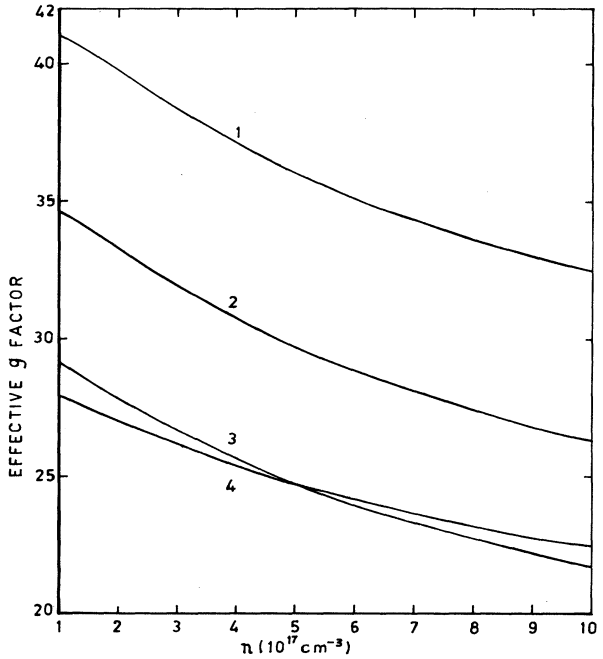

FIG. 2. Effective g factor (magnitudes only) vs carrier concentration for (1) p-type $Pb_{1-x}Mn_xSe$ at $x=0.01$; (2) p-type $Pb_{1-x}Mn_xSe$ at $x=0.005$; (3) n-type $Pb_{1-x}Mn_xSe$ at $x=0.005$; (4) n-type $Pb_{1-x}Mn_xSe$ at $x=0.02$, at $T=4.2$ K.

In Table II, we have listed our calculated band edge g values in $Pb_{1-x}Mn_xTe$. The variation of the effective g factor as a function of x shows that it increases with x for the valence band and decreases with an increase in x for the conduction band. These trends are as found in the $Pb_{1-x}Mn_xSe$ case. Therefore, we believe that our results are reasonable despite lack of experimental results for

TABLE I. Band edge effective g factors for $Pb_{1-x}Mn_xSe$ (only magnitudes). Top: Valence band (4.2 K). Bottom: Conduction band (4.2 K).

x	g (Without exchange)	g (Exchange contribution)	g (With exchange)	g (Expt.) (Ref. 17)
0	31.635	0	31.635	31
0.005	28.042	6.376	34.419	
0.0063	27.230	8.034	35.265	34.923
0.01	25.143	12.752	37.895	38.615
0.015	21.633	19.129	40.762	
0.0175	22.284	22.317	43.451	
0.02	20.656	25.505	46.161	
0	32.784	0	32.784	32
0.005	29.192	−0.708	28.483	
0.0063	28.380	−0.893	27.487	27.46
0.01	26.292	−1.417	24.875	23.846
0.015	22.782	−2.125	20.657	
0.0175	22.284	−2.480	19.804	
0.02	21.806	−2.834	18.972	

TABLE II. Band edge effective g factors for $Pb_{1-x}Mn_xTe$ (only magnitudes). Top: Valence band (30 K). Bottom: Conduction band (30 K).

x	g (Without exchange)	g (Exchange contribution)	g (With exchange)	g (Ref. 46) (Expt.)
0	25.769	0	25.769	29.23
0.005	22.414	5.045	27.463	
0.01	19.734	10.099	29.834	
0.015	17.545	15.150	32.695	
0.02	15.722	20.199	35.922	
0	26.063	0	26.063	29.16
0.005	22.708	−3.254	19.453	
0.01	20.028	−6.509	13.519	
0.015	17.839	−9.763	8.076	
0.02	16.017	−13.017	2.999	

comparison. A careful analysis of the results shows that the exchange contribution to the g factor becomes significant as x increases. As in the case of PbMnSe, here also the exchange contributions are positive in the case of the valence band and $-ve$ for the conduction band. In order to test the accuracy of results and chosen experimental exchange parameters, we calculate, in the next section, the effective masses and their anisotropies in $Pb_{1-x}Mn_xTe$ and $Pb_{1-x}Mn_xSe$ and compare them with available experimental results.

IV. EFFECTIVE MASSES IN $Pb_{1-x}Mn_xTe$ AND $Pb_{1-x}Mn_xSe$

In this section, we shall calculate the effective masses and mass anisotropies in the lead-salt-based diluted magnetic semiconductors. Using perturbation theory, we have

$$\mathcal{E}_{c,v}(\mathbf{k})=E_{c,v}(\mathbf{k})+\langle c,v|\mathcal{H}_{\rm ex}|c,v\rangle + \sum_{m\neq c,v}\frac{|\langle c,v|\mathcal{H}_{\rm ex}|m\rangle|^2}{E_{c,v}-E_m}\ , \tag{4.1}$$

where $\mathcal{E}_{c,v}(\mathbf{k})$ is the total energy of the conduction and valence bands including the exchange interaction. Using Eqs. (2.2) and (3.2), and Eqs. (3.7) and (3.8) of Ref. 20 for the wave functions and energies in Eq. (4.1), we obtain, after a straightforward algebra, the conduction-band energy

$$\begin{aligned}\mathcal{E}_c(\mathbf{k})=&\epsilon_2^- +\frac{\hbar^2k^2}{2m}+\frac{1}{2}E_G(W-1)+M_{1c}k_\rho^2+M_{2c}k_z^2+\left[\frac{M_{3c}}{W(1+W)}+\frac{M_{4c}}{W}\right]k_\rho^4+\left[\frac{M_{5c}}{W(1+W)}+\frac{M_{6c}}{W}\right]k_z^4\\&+\left[\frac{M_{7c}}{W(1+W)}+\frac{M_{8c}}{W}\right]k_\rho^2k_z^2+\tfrac{1}{2}xN_s\langle S^z\rangle\left[\left[\frac{1+W}{2W}\right]B'+2\frac{\hbar^2}{m^2}\frac{A'}{E_G^2W(1+W)}(t^2k_z^2-\tfrac{1}{2}s^2k_\rho^2)\right]\\&+\frac{1}{4}\frac{\hbar^2}{m^2}\frac{x^2N_s^2\langle S^z\rangle^2}{E_G^3W^3}[t^2k_z^2(B'-A')^2+\tfrac{1}{2}s^2k_\rho^2(A'+B')^2]\ .\end{aligned} \tag{4.2}$$

The expression for the valence-band energy $\mathcal{E}_v(\mathbf{k})$ can be obtained by replacing ϵ_2^- by ϵ_1^+ in the first term, the $+$ sign by the $-$ sign in the third term, the index c by v and by interchanging A' and B' in Eq. (4.2). The longitudinal and transverse effective masses, $m_{c,v}^l$ and $m_{c,v}^t$, are obtained by the following formulas:

$$\frac{1}{m_{c,v}^l}=\frac{2\partial\mathcal{E}_{c,v}(k_\rho^2,k_z)}{\hbar^2\partial k_z^2}\bigg|_{k_\rho^2=0,k_z=k_l} \tag{4.3}$$

and

$$\frac{1}{m_{c,v}^t}=\frac{2\partial\mathcal{E}_{c,v}(k_\rho^2,k_z)}{\hbar^2\partial k_\rho^2}\bigg|_{k_\rho^2=0,k_z=k_l}\ . \tag{4.4}$$

From Eqs. (4.2)–(4.4), we obtain

$$\begin{aligned}\frac{1}{m_c^l}=&1+\frac{\beta E_G}{2W}+2M_{2c}+\frac{k_l^3}{W^3}\left[4W^2\left[\frac{M_{5c}}{1+W}+M_{6c}\right]-\beta k_l^2\left[\frac{1+2W}{(1+W)^2}M_{5c}+M_{6c}\right]\right]\\&-\frac{1}{2}\frac{xN_s\langle S^z\rangle}{W^3}\left[\frac{\beta B'}{2}+\frac{2A'}{E_G^2}\left\{\frac{\beta(1+2W)t^2k_l^2}{(1+W)^2}-\frac{2t^2W^2}{1+W}\right\}\right]\\&+\frac{1}{4}\frac{x^2N_s^2\langle S^z\rangle^2}{W^5E_G^3}[2t^2W^2(B'-A')^2-2\beta(B'-A')^2t^2k_l^2]\end{aligned} \tag{4.5}$$

and

$$\begin{aligned}\frac{1}{m_c^t}=&1+\frac{\alpha E_G}{2W}+2M_{1c}-\frac{\alpha k_l^4}{W^3}\left[\frac{1+2W}{(1+W)^2}M_{5c}+M_{6c}\right]+2\frac{k_l^2}{W}\left[\frac{M_{7c}}{1+W}+M_{8c}\right]\\&-\frac{1}{2}\frac{xN_s\langle S^z\rangle}{W^3}\left[\frac{\alpha B'}{2}+\frac{2A'}{E_G^2}\left\{\frac{s^2W^2}{1+W}+\frac{\alpha(1+2W)}{(1+W)^2}t^2k_l^2\right\}\right]\\&+\frac{1}{4}\frac{x^2N_s^2\langle S^z\rangle^2}{E_G^3W^5}[(A'+B')^2s^2W^2-3(B'-A')^2t^2k_l^2]\ .\end{aligned} \tag{4.6}$$

The corresponding quantities for the valence band are obtained by changing E_G to $-E_G$, replacing c by v, and interchanging A' and B' in Eqs. (4.5) and (4.6). In Eqs. (4.5) and (4.6), $W=\sqrt{1+\beta k_l^2}$.

In order to compare with experiment, we calculate the anisotropy of the cyclotron effective masses, which are given by[40]

$$K_{c,v}^{q}=\frac{m_{c,v}^{l}[1+\Delta_{c,v}^{t}\mu_{c,v}/E_G]}{m_{c,v}^{t}[1+\Delta_{c,v}^{l}\mu_{c,v}/E_G]}\ , \tag{4.7}$$

where

$$\Delta_{c,v}^{l}=m_{c,v}^{l0}\left[\frac{1}{m_{c,v}^{lf}}-\frac{1}{m_{v,c}^{lf}}\right] \tag{4.8}$$

and

$$\Delta_{c,v}^{t}=m_{c,v}^{t0}\left[\frac{1}{m_{c,v}^{tf}}-\frac{1}{m_{v,c}^{tf}}\right]\ . \tag{4.9}$$

In Eqs. (4.7)–(4.9), $m_{c,v}^{l}$ and $m_{c,v}^{t}$ are the longitudinal and transverse effective masses for the conduction (c) and valence (v) bands, respectively. The superscripts 0 and f denote the contribution due to band edge and the far bands including the free carrier contributions, respectively. μ_c is the chemical potential for the n-type system and μ_v for the p-type system.

We have plotted the band edge transverse effective masses of electrons and holes in Fig. 3 as functions of Mn concentration. For p types of $Pb_{1-x}Mn_xTe$, the agreement with experiment[16] is good. However, for n-type $Pb_{1-x}Mn_xTe$, the experimental values[41] are somewhat less than our values. Within experimental errors, we believe the agreement between our calculations and the experiments is reasonably fair. In contrast to the effective g factors, where the exchange interactions are significant, in the case of effective masses, the exchange contribution accounts for only less than 5% of the nonexchange value. This is due presumably to the fact that the effective g factors are affected significantly by the magnetic polarization due to impurity atoms, while the effective masses are not. In Fig. 4, we have plotted the cyclotron mass anisotropies as functions of carrier density for different values of x. It is observed that, for a fixed x, the mass anisotropy increases in p-type $Pb_{1-x}Mn_xTe$ and decreases in n-type $Pb_{1-x}Mn_xTe$. However, for a fixed carrier density, the mass anisotropy increases with x. Our results for $x=0$ in both n- and p-type $Pb_{1-x}Mn_xTe$ are in good agreement with experimental results.[42–48]

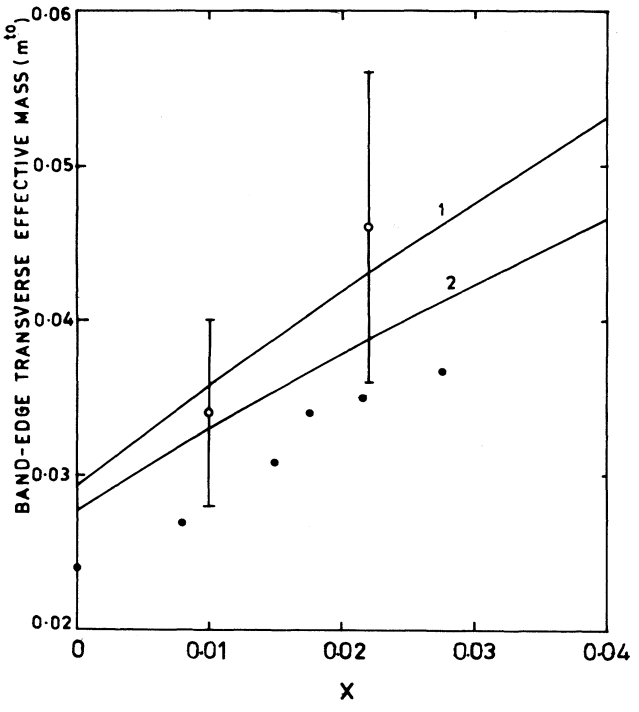

FIG. 3. Band edge transverse effective mass (magnitudes only) vs manganese concentration at $T=30$ K for (1) p-type $Pb_{1-x}Mn_xTe$ and (2) n-type $Pb_{1-x}Mn_xTe$. Open circles (○) denote experimental points (Ref. 16) for p-type $Pb_{1-x}Mn_xTe$ and solid circles (●) for n-type $Pb_{1-x}Mn_xTe$ (Ref. 41).

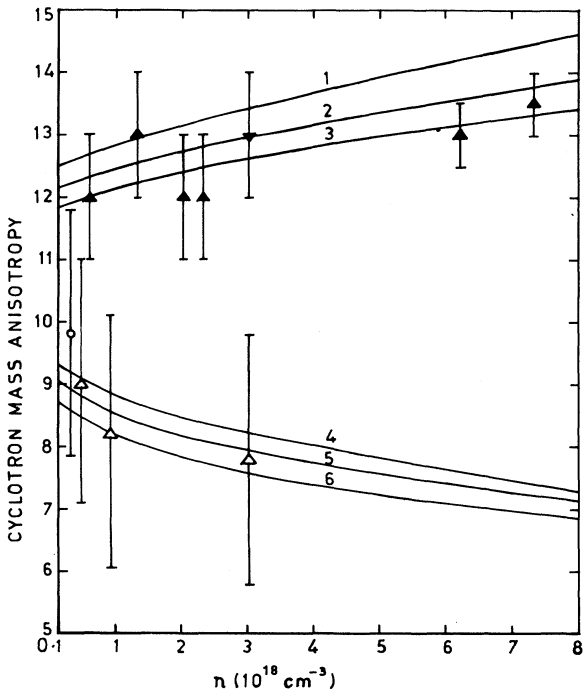

FIG. 4. Cyclotron mass anisotropy vs carrier concentrations for p-type $Pb_{1-x}Mn_xTe$ at $x=0.02$ (curve 1), $x=0.01$ (curve 2), and $x=0.0$ (curve 3), respectively, and for n-type $Pb_{1-x}Mn_xTe$ at $x=0.02$ (curve 4), $x=0.01$ (curve 5), and $x=0.0$ (curve 6), respectively. The curves for finite x values are plotted for $T=30$ K. ▲ (Ref. 45) and ▼ (Ref. 44) represent experimental points for p-type $Pb_{1-x}Mn_xTe$ ($x=0.0$) and △ (Ref. 43) and ○ (Ref. 46) represent experimental points for n-type $Pb_{1-x}Mn_xTe$ ($x=0.0$).

V. SUMMARY AND CONCLUSION

This work presents a systematic derivation of an expression for the effective g factor in solids in the presence

of magnetic impurities. The expression is suitably modified so as to make it applicable to the diluted magnetic semiconductors. As an example, we calculated the effective g factors in $Pb_{1-x}Mn_xSe$ and $Pb_{1-x}Mn_xTe$. The calculations are based on a $\mathbf{k}\cdot\boldsymbol{\pi}$ band model developed and used by us in our previous works. Apart from the band edge g values, the g values were calculated as functions of carrier concentrations and magnetic impurity concentration. The agreement with experiment where available is good. We have also derived the effective masses for the afore-mentioned systems. The cyclotron mass anisotropy was calculated and studied by varying the carrier concentration and magnetic impurity. It was found that while the exchange interaction between the carriers and magnetic impurities contributes significantly to the effective g factor, its effect is small on the effective masses. This is due presumably to the reason that, while the exchange interaction affects drastically the polarization of carriers in the presence of a magnetic field, thus contributing significantly to the effective g factor, its effect is less on an electronic parameter like the effective mass. We have compared our results with experiment where available and within the experimental errors our calculations agree well with experimental results.

In conclusion, we would like to state that in this work we have made a serious effort to calculate and analyze the effective g factors and effective masses in the IV–VI-based diluted magnetic semiconductors. However, our derivation of the effective g factor is general in the sense that it can be applied to other diluted magnetic semiconductors, with suitable modifications.

ACKNOWLEDGMENT

This work was supported by the University Grants Commission, New Delhi through a research grant to one of the authors (G.S.T.).

APPENDIX

Here we present an alternative derivation of the effective g factor from the expression for the spin Knight shift[31,32] at the jth nuclear site

$$K_{js}^{\nu\mu}=K_{js\,\mathrm{cond}}^{\nu\mu}+K_{js\,\mathrm{loc}}^{\nu\mu}\ , \tag{A1}$$

where

$$K_{js}^{\nu\mu}=-\tfrac{1}{2}\mu_0\sum_{\mathbf{k}}X_{jn\rho,n\rho'}^{\nu}g_{nn}^{\mu}(\mathbf{k})\sigma_{n\rho',n\rho}^{\mu}f'(E_{n\mathbf{k}}) \tag{A2}$$

with

$$\mathbf{X}_j=\frac{8\pi}{3}\boldsymbol{\sigma}\delta(\mathbf{r}_j)+\left[-\frac{\boldsymbol{\sigma}}{r_j^3}+\frac{3(\boldsymbol{\sigma}\cdot\mathbf{r}_j)\mathbf{r}_j}{r_j^5}+\frac{2r_j(\boldsymbol{\pi}+e\,\mathbf{A}/c)}{\hbar r_j^3}\right] \tag{A3}$$

and

$$K_{j\,\mathrm{loc}}^{\nu\mu}=\frac{(g_i-1)A_{ji}^{\nu\nu'}\chi_i^{\nu'\mu}}{\mu_0 g_i\gamma_j\hbar}\ . \tag{A4}$$

In Eq. (A4) repeated indices imply summation. $A_{ji}^{\nu\nu'}$ is the indirect exchange interaction coupling between the nucleus at the jth site and the magnetic impurity at the ith site and is given by

$$A_{ji}^{\nu\nu'}=\frac{g_j\mu_0^3\gamma_j\hbar}{g_i-1}\sum_{\mathbf{k},\mathbf{k}'}\left[X_{n\mathbf{k}\rho,n'\mathbf{k}'\rho'}^{\nu}X_{n'\mathbf{k}'\rho',n\mathbf{k}\rho}^{\nu'}\times e^{-i(\mathbf{k}-\mathbf{k}')\cdot\mathbf{R}_{ji}}+\mathrm{c.c.}\right]\times\frac{f(E_{n\mathbf{k}})}{E_{n'\mathbf{k}'}-E_{n\mathbf{k}}}\ , \tag{A5}$$

$\chi_i^{\nu'\mu}$ is the Curie-Weiss susceptibility tensor of the impurity at site i, γ_j is the nuclear gyromagnetic ratio, and g_i is the g factor of the impurity atom.

Since we are interested only in the intraband g factor and the term in Eq. (A5) for which $\mathbf{k}=\mathbf{k}'$, we have, after a little algebra,

$$A_{ji}^{\nu\nu'}=-\frac{g_i\mu_0^3\gamma_j\hbar}{g_i-1}\sum_{\mathbf{k}}X_{jn\rho,n\rho'}^{\nu}X_{in\rho',n\rho}^{\nu'}f'(E_{n\mathbf{k}})\ . \tag{A6}$$

From Eqs. (A1), (A2), (A4), and (A6) we obtain

$$K_{js}^{\nu\mu}=-\tfrac{1}{2}\mu_0\sum_{\mathbf{k}}X_{jn\rho,n\rho'}^{\nu}\times[g_{nn}^{\mu}(\mathbf{k})\sigma_{n\rho',n\rho}^{\mu}+2X_{in\rho',n\rho}^{\nu'}\chi_i^{\nu\mu}]\times f'(E_{n\mathbf{k}})\ , \tag{A7}$$

from which we obtain the effective g factor

$$g_{nn}^{\mathrm{eff},\mu}=g_{nn,0}^{\mathrm{eff},\mu}+2X_{in\rho,n\rho}^{\nu'}\chi_i^{\nu'\mu}\ , \tag{A8}$$

where $g_{nn,0}^{\mathrm{eff},\mu}$ denotes the first term in the square bracket of Eq. (A7) and is given by[30]

$$g_{nn,0}^{\mathrm{eff},\mu}(\mathbf{k})=g\sigma_{n\rho,n\rho}^{\mu}+\frac{2i}{m}\epsilon_{\alpha\beta\mu}\sum_{\substack{m,\rho'\\ m\neq n}}\frac{\pi_{n\rho,m\rho'}^{\alpha}\pi_{m\rho',n\rho}^{\beta}}{E_{mn}}\ , \tag{A9}$$

and in the second term of Eq. (A8) we have considered the diagonal matrix element of $X_i^{\nu'}$ both in band and spin indices. Assuming

$$\chi_i^{\nu'\mu}=\chi_i^{\nu'\nu'}\delta_{\nu'\mu}\ , \tag{A10}$$

the second term of Eq. (A8), which we denote as $g_{nn,i}^{\mathrm{eff},\mu}$, becomes

$$g_{nn,i}^{\mathrm{eff},\mu}(\mathbf{k})=\frac{2}{B^{\mu}}X_{in\rho,n\rho}^{\mu}\langle M_i^{\mu}\rangle\ , \tag{A11}$$

where we have used the relation

$$\chi_i^{\mu\mu}=\frac{\langle M_i^{\mu}\rangle}{B^{\mu}}\ . \tag{A12}$$

Now

$$\langle M_i^{\mu}\rangle=-g_i\mu_0\langle J_i^{\mu}\rangle\ , \tag{A13}$$

and assuming only the contact type of interaction between the electron spin and the magnetic impurity spin, we have

$$X_i^{\mu}=\frac{8\pi}{3}\sigma^{\mu}\delta(\mathbf{r}-\mathbf{R}_i)\ . \tag{A14}$$

Using Eqs. (A12)–(A14) in Eq. (A11), we obtain

$$g_{nn,i}^{\text{eff},\mu}(\mathbf{k})=\frac{1}{\mu_0 B^{\mu}}N_i\langle J_i^{\mu}\rangle\left[-\frac{8\pi}{3}g_i\mu_0^2 2\sigma^{\mu}\delta(\mathbf{r}_i)\right]_{n\rho,n\rho}, \tag{A15}$$

where N_i is the number of impurity atoms which we can express as $N_i=xN_s$. N_s being the number of unit cells per unit volume. Equation (A15) can now be written as

$$g_{nn,i}^{\text{eff},\mu}(\mathbf{k})=\frac{xN_s\langle J^{\mu}\rangle}{\mu_0 B^{\mu}}[\sigma^{\mu}\mathcal{J}(r)]_{n\rho,n\rho}\ , \tag{A16}$$

where

$$\mathcal{J}(\mathbf{r})=-\frac{16\pi}{3}g_i\mu_0^2\delta(\mathbf{r})\ . \tag{A17}$$

Equation (A16) is same as Eq. (2.21). Thus, we have derived the effective g factor from the expression for the Knight shift in the presence of magnetic impurities.

[1]M. N. Vinogradova, N. V. Kolomeets, and L. M. Sysoeva, Fiz. Tekh. Poluprovodn. **5**, 218 (1971) [Sov. Phys. Semiconductors **5**, 186 (1971)].

[2]N. B. Brandt and V. V. Moshchalkov, Adv. Phys. **33**, 193 (1984).

[3]J. K. Furdyna, J. Appl. Phys. **64**, R29 (1988).

[4]G. Bauer, in *Diluted Magnetic Semiconductors,* edited by R. L. Aggarwal, J. K. Furdyna, and S. Von Molnar, MRS Symposia Proceedings No. 89 (Materials Research Society, Pittsburgh, 1987), p. 187.

[5]W. Giriat and J. K. Furdyna, in *Semiconductors and Semimetals,* edited by R. K. Willardson, and A. C. Beer, J. K. Furdyna and J. Kossut, (Academic, Boston, 1988), Vol. 25, p. 1.

[6]J. Niewodniczanska-Zawadzka and A. Szczerbakow, Solid State Commun. **34**, 887 (1980).

[7]M. Escorne, A. Mauger, J. L. Tholence, and R. Triboulet, Phys. Rev. B **29**, 6306 (1984).

[8]J. R. Anderson and M. Gorska, Solid State Commun. **52**, 601 (1984).

[9]H. Pascher, E. J. Fanter, G. Bauer, W. Zawadzki, and M. V. Ortenberg, Solid State Commun. **48**, 461 (1983).

[10]G. Karczewski, M. Von Ortenberg, Z. Wilamowski, W. Dobrowolski and J. Niewodniczanska-Zawadzka, Solid State Commun. **55**, 249 (1985).

[11]A. Bruno, J. P. Lascaray, M. Averous, J. M. Broto, J. C. Ousset, and J. F. Dumas, Phys. Rev. B **35**, 2068 (1987).

[12]G. Braunstein, G. Dresselhaus, J. Heremans, and D. Partin, Phys. Rev. B **35**, 1969 (1987).

[13]M. Gorska and J. R. Anderson, Phys. Rev. B **38**, 9120 (1988).

[14]C. W. H. M. Vennix, E. Frikee, H. J. M. Swagten, K. Kopinga, and W. J. M. de Jonge, J. Appl. Phys. **69**, 6025 (1991).

[15]T. Story, C. H. W. Swuste, H. J. M. Swagten, and R. J. T. Van Kempen, J. Appl. Phys. **69**, 6037 (1991).

[16]M. Gorska, T. Wojtowicz, and W. Knap, Solid State Commun. **51**, 115 (1984).

[17]L. Kowalczyk, Semicond. Sci. Technol. **6**, 115 (1991).

[18]L. Liu and G. Bastard, Phys. Rev. B **25**, 487 (1982).

[19]M. Von Ortenberg, Solid State Commun. **52**, 111 (1984).

[20]R. L. Hota and G. S. Tripathi, J. Phys.: Condens. Matter **3**, 6299 (1991).

[21]L. M. Roth, Phys. Rev. **188**, 1534 (1960).

[22]H. J. Zeiger and G. W. Pratt, *Magnetic Interactions in Solids* (Clarendon, Oxford, 1973), p. 377.

[23]G. Bastard, C. Rigaux, Y. Guldner, A. Mycielski, J. K. Furdyna, and D. P. Mullin, Phys. Rev. B **24**, 1961 (1981).

[24]J. K. Furdyna, J. Appl. Phys. **53**, 7637 (1982).

[25]D. Heiman, P. A. Wolff, and J. Warnock, Phys. Rev. B **27**, 4848 (1983).

[26]P. Byszewski, K. Szlenk, J. Kossut, and R. R. Galazka, Phys. Status Solidi B **95**, 359 (1979).

[27]M. Dobrowolska, W. Dobrowolski, R. R. Galazka, and J. Kossut, Solid State Commun. **28**, 25 (1979).

[28]W. Dobrowolski, M. Von Ortenberg, J. Thielman, and R. R. Galazka, Phys. Rev. Lett. **47**, 541 (1981).

[29]P. K. Misra and L. Kleinman, Phys. Rev. B **5**, 4581 (1972).

[30]G. S. Tripathi, L. K. Das, P. K. Misra, and S. D. Mahanti, Phys. Rev. B **25**, 3091 (1982).

[31]G. S. Tripathi, J. Phys. C **18**, L1157 (1985).

[32]G. S. Tripathi, B. Mishra, and P. K. Misra, J. Magn. Magn. Mater. **67**, 271 (1987).

[33]D. L. Mitchell and R. F. Wallis, Phys. Rev. **151**, 581 (1966).

[34]R. L. Bernick and L. Kleinman, Solid State Commun. **8**, 569 (1970).

[35]S. Misra, G. S. Tripathi, and P, K. Mirsa, J. Phys. C **17**, 869 (1984); **19**, 2007 (1986); **20**, 277 (1987).

[36]C. M. Misra and G. S. Tripathi, Phys. Rev. B **40**, 11 168 (1989).

[37]R. L. Hota and G. S. Tripathi, Phys. Rev. B **44**, 1918 (1991); **45**, 10 783 (1992).

[38]L. Kleinman (private communication).

[39]J. Niewodniczanska-Zawadzka, J. Kossut, A. Sandauer, and W. Dobrowolski, in *Physics of Narrow Gap Semiconductors,* edited by W. Zawadzki, Lecture Notes in Physics Vol. 152 (Springer-Verlag, Berlin, 1982), p. 326.

[40]G. Nimitz and B. Schlicht, in *Narrow Gap Semiconductors,* Springer Tracts in Modern Physics Vol. 98 (Springer, Berlin, 1983).

[41]J. Niewodniczanska-Zawadzka, G. Elsinger, L. Palmetshofer, A. Lopez-Otero, E. J. Fantner, G. Bauer, and W. Zawadzki, Physica B **117-118**, 458 (1983).

[42]G. M. T. Foley and D. N. Langenberg, Phys. Rev. B **15**, 4850 (1977).

[43]M. Fujimoto, J. Phys. Soc. Jpn. **21**, 1706 (1966).

[44]J. R. Burke, B. Houston, and H. T. Savage, Phys. Rev. B **2**, 1977 (1970).

[45]J. D. Jensen, B. Houston, and J. R. Burke (unpublished).

[46]R. Nil, J. Phys. Soc. Jpn. **19**, 58 (1964); R. Nil and A. Kobayashi, *Plasma Effects in Solids* (Dunod, Paris, 1964), p. 65; H. Numata and Y. Uemura, J. Phys. Soc. Jpn. **19**, 2140 (1964).

[47]T. E. Thompson, P. R. Aron, B. S. Chandrasekhar, and D. N. Langenberg, Phys. Rev. B **4**, 518 (1971).

[48]C. K. N. Patel and R. E. Slusher, Phys. Rev. **177**, 1200 (1969).